High Precision Motion Control of Parallel Robots with Imperfections and Manufacturing Tolerances

Islam S. M. Khalil, E. Globovic and Asif Sabanovic

Faculty of Engineering and Natural Sciences
Sabanci University
Tuzla Campus - Orhanli 34956 Istanbul, Turkey
kahalil, edin, asif@sabanciuniv.edu

Abstract—This work attempts to achieve precise motion control using parallel robots with manufacturing tolerances and inaccuracies by migrating the measurements from their joint space to task space in order to decrease control system's sensitivity to any kinematical uncertainty rather than calibrating the parallel plant. The problem of dynamical model uncertainties and its effect on the derivation of the control law is also addressed in this work through disturbance estimation and compensation. Eventually, both task space measurement and disturbance estimation are combined to formulate a control framework that is unsensitive to either kinematical and dynamical system uncertainties.

Keywords—Task space measurement, disturbance rejection, kinematical inaccuracies.

I. INTRODUCTION

In the area of robotics, development of parallel manipulators is driven by the crucial need for accurate, rigid and highly responsive mechanisms. Rigidity is naturally guaranteed by the closed structure of such parallel manipulators. Consequently, the obtained rigidity allows performing operations at high acceleration levels without subjecting the end effector to any residual vibrations. However, accuracy and precision of such systems relay on numerous factors that can deteriorate the performance of such systems such as complicity of their mechanical structure that is not often modeled while driving the motion control law. In addition, the presence of numerous passive joints results in undesired clearances and therefore lack of accuracy [1]. Moreover, assembly errors along with thermal deformations contribute in deteriorating parallel mechanisms accuracy. Nevertheless, accuracy of parallel robots can be examined through periodic kinematical calibration that provides a measure for how accurate the map between joint and task space is. Much work has been expended by researchers to guarantee accurate mapping between joint and task spaces. An error model was built in [2] which takes the geometric errors into account by using a 3D coordinate measuring machine for making a constraint conditions to obtain a calibration equation in the workspace. However the work require using the 3D coordinate measuring machine. In [4], a relation between the joint displacement error of a parallel manipulator and the end effector accuracy was presented. In addition, position error of the joints, the actuation error and the backlash are included in the kinematic model. A two stage calibration procedure for Delta robot was presented in [5], which allows identifying the offsets on the three joints and the absolute location of the robot base using a displacement sensor and dedicated target that can be moved on the work area. Two methods for calibrating a planar parallel robot were presented in [6], geometric error iterative method and a nonlinear fitting method to calibrate the home position of the parallel robot. A novel method for parallel robot's pose measurement and calibration was introduced in [7] using a three planes measuring method, In addition, a kinematical model of a parallel robot with parallel tracks and LSM is adopted for calibration of robot's geometrical parameters. This work attempts to achieve precise motion control using a parallel robot that encounters manufacturing tolerances, assembly errors and thermal deformations without periodic calibration through migrating the joint space measurements to task space in order to decrease the sensitivity of the control system to any kinematical uncertainties whatsoever. On the other hand, dynamical uncertainties such as the unmodeled dynamics are considered as disturbances, then a disturbance observer is designed to estimate such disturbances and used to generate a compensating control law [8]. Migrating the measurement to the task space along with disturbance estimation and compensation allows performing motion control on parallel robots regardless to both kinematical and dynamical uncertainties. The proposed framework is analyzed and implemented on a pantograph mechanism to verify the validity of the proposed technique. This paper is organized as follows, Section II presents the problem formulation where error analysis is performed for both systems with task space and joint space measurements. Section III includes derivation of the motion control law for both cases. Experimental results are included in section IV, where experiments are conducted on a pantograph mechanism using both configuration and task space measurements. Eventually, final remarks and conclusions are included in section V.

II. ERROR ANALYSIS

A. Joint space measurement

Figure. 1 illustrates the block diagram representation of the control system when measurements are taken from the joint space. Therefore, the error between the desired time varying reference of the end effector $r(s)$ and the measured output

$C(s)$ can be expressed as follows

$$\xi(s) = r(s) - C(s) \tag{1}$$

since, the output can be expressed as

$$C(s) = P(s)R(s)\frac{G(s)}{1 + G(s)} \tag{2}$$

where, $G(s)$ is the transfer function of the controller and the actuators while $P(s)$ is the transfer function of the linearized parallel plant. $R(s)$ is the time varying reference in the joint space that is related to the desired end effector reference position through the following nonlinear kinematical relation

$$R(s) = \Psi(r(s)) \tag{3}$$

where, Ψ is a nonlinear map between the joint and task space for a given parallel robot. Consequently, $\xi(s)$ can be expressed as follows

$$\xi(s) = \frac{r(s)(1 + G(s)) - \Psi(r(s))P(s)G(s)}{1 + G(s)} \tag{4}$$

Assuming stability of the system, we can write

$$\xi_{ss}(s) = \lim_{t \to \infty} \xi(t) = \lim_{s \to 0} s\, \xi(s) \tag{5}$$

Therefore, steady state error can be written as

$$\xi_{ss}(s) = \lim_{s \to 0} s\, \frac{r(s)(1 + G(s)) - \Psi(r(s)P(s)G(s))}{1 + G(s)} \tag{6}$$

which in turn implies that a steady state error will exist in the final response due to the kinematical inaccuracies. In other words, if $r(s) = \frac{1}{s}$, a unit steady state error will appear in the final response.

$$\xi_{ss}(s) = \lim_{s \to 0} s\, \frac{\frac{1}{s}(1 + G(s)) - \Psi(\frac{1}{s})P(s)G(s)}{1 + G(s)} = 1 . \tag{7}$$

Equation (7) indicates that the controller has no effect on the steady state error due to the nature of the measurement, where the parallel robot is placed out of the control loop. Therefore, all the kinematical inaccuracies will definitely contribute in deteriorating the joint-task space mapping which in turn deteriorate the overall accuracy of the system.

B. Task space measurement

Migrating the measurements from the joint to task space of the system results in including the parallel robot into the closed loop of the control system as depicted in Fig.2. Similarly, $C(s)$ can be expressed as

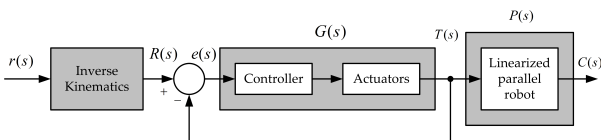$$C(s) = r(s)\frac{G(s)P(s)}{1 + G(s)P(s)} \tag{8}$$
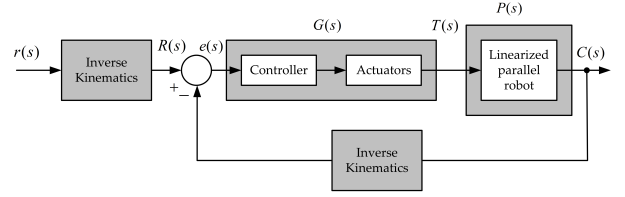

Fig. 1.   Joint space measurement.

Fig. 2.   Task space measurement.

since,

$$\frac{\xi(s)}{r(s)} = 1 - \frac{G(s)P(s)}{1 + G(s)P(s)} \tag{9}$$

therefore,

$$\xi(s) = r(s)\frac{1}{1 + G(s)P(s)} \tag{10}$$

Consequently, the steady state error can be expressed as

$$\xi_{ss}(s) = \lim_{s \to 0} s\, \frac{r(s)}{1 + G(s)P(s)} . \tag{11}$$

Unlike equation (7), (11) indicates that the control action can minimize the steady state error in the final response as a result of migrating the parallel plant inside the closed control loop. In other words, all the kinematical inaccuracies including manufacturing tolerances, assembly errors, thermal deformations,.etc are no longer outside the control loop that naturally becomes relatively less sensitive to these errors compared with the joint space measurement configuration.

III. PLANAR PANTOGRAPH PARALLEL ROBOT

A. Pantograph kinematics and uncertainties

The Pantograph's configuration level kinematics can be written as follows taking the kinematical uncertainties into consideration

$$\begin{aligned} x &= (l_1 + \Delta l_1)\cos q_1 + (l_2 + \Delta l_2)\cos q_2 \\ y &= (l_1 + \Delta l_1)\sin q_1 + (l_2 + \Delta l_2)\sin q_2 \end{aligned} \tag{12}$$

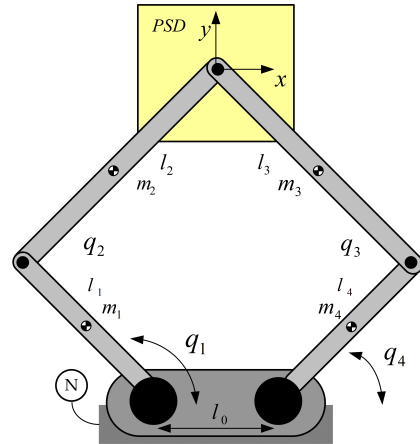Fig. 3.   Pantograph configuration.

where, q_1 and q_4 are the active angles of the pantograph, while q_2 and q_3 are its passive angles. x and y are the coordinates of the task space. Δl_i is the kinematical uncertainty associated with the ith link due to manufacturing tolerances, assembly errors, thermal deformations and many other factors that cannot be negligible when precise motion control is required to be accomplished in the task space. Consequently, the motion level kinematics can be obtained by taking the time derivative of (12) with respect to the Newtonian frame N as illustrated in Fig.3, therefore the kinematical jacobian is

$$\mathrm{J} = \begin{bmatrix} -(l_1 + \Delta l_1)\sin q_1 & -(l_2 + \Delta l_2)\sin q_2 \\ (l_1 + \Delta l_1)\cos q_1 & (l_2 + \Delta l_2)\cos q_2 \end{bmatrix} \qquad (13)$$

the motion level kinematic map can be written as follows

$$\underline{\dot{\mathrm{x}}} = \mathrm{J}\,\underline{\dot{\mathrm{q}}} \qquad (14)$$

that can be integrated to obtain the inverse kinematic relation. However, integration of (14) can result in increasing any initial error with time. Therefore, feedback stabilization approach is used to guarantee that integration of (14) will not magnify the initial error. Introducing the following lyapnouv function

$$\mathrm{V}(t) = \mathrm{e}^{\mathrm{T}}\mathrm{e} \qquad (15)$$

where, e is the error between the right and left hand side of (12), which can be expressed as follows

$$e = \underline{\mathrm{x}} - \Phi(\underline{\mathrm{q}}) \qquad (16)$$

taking the time derivative of the lyapnouv function we obtain

$$\dot{\mathrm{V}}(t) = 2\mathrm{e}\dot{\mathrm{e}} = -2\mathrm{e}\frac{d\Phi(\underline{\mathrm{q}})}{dt} = -2\mathrm{e}\,\mathrm{J}\,\underline{\dot{\mathrm{q}}} \qquad (17)$$

selecting $\underline{\dot{\mathrm{q}}}$ as $\mathrm{J}^{-1}\mathrm{ke}$, where $\mathrm{k} \in \mathrm{R}^+$ that in turn guarantees the exponential stability as $\dot{\mathrm{V}} = -2\mathrm{ke}^2 < 0$. Implementation of the previous equation is illustrated in Fig.4 where pantograph's end effector position is measured from the task space rather than having it through a kinematical map from the joint space. A position sensing device can be used for this purpose. Figure. 4 illustrates the implementation of the previous inverse kinematics stabilization integration based method, where the inverse kinematics has to be performed on the reference input along with the pantograph's end effector position measured from the task space using a PSD sensor. Although end effector's actual position is measured, transforming the task space coordinates ($\underline{\mathrm{x}}$) to the joint space coordinates ($\underline{\mathrm{q}}$) adds some error e_k due to the kinematical uncertainties in (12) and
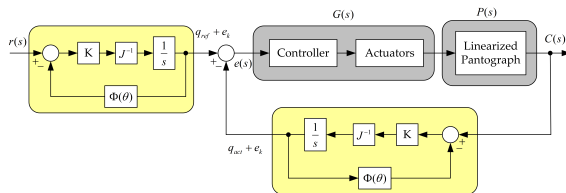

Fig. 4. Task space measurement.

(13). Nevertheless, these errors will cancel out when the error signal $e(s)$ is computed as follows

$$e(s) = q_{ref} + e_k - (q_{act} + e_k) \qquad (18)$$

Therefore, the control system naturally becomes insensitive to the kinematical errors that experience has proven to be neither avoidable nor negligible. In addition, the previous process not only keeps the control system insensitive to the kinematical inaccuracies but also makes periodic calibration unnecessary.

B. Pantograph dynamics and uncertainties

1) Configuration space measurements: The pantograph's dynamical equation of motion in the configuration space can be written as follows

$$M(q)\ddot{q} + b(q,\dot{q}) + g(q) = \tau(t) \qquad (19)$$

where, $M(q)$ is the pantograph's positive definite inertia matrix, $b(q,\dot{q})$ is a vector of coriolis and centripetal forces, $g(q)$ is the gravity term while $\tau(t)$ is the generalized torque vector acting on the generalized coordinate vector q. Taking the dynamical inaccuracies into consideration, one can write the following relations

$$M(q) = M_n(q) + \Delta M(q) \ , \ g(q) = g_n(q) + \Delta g(q)$$

$$b(q,\dot{q}) = b_n(q,\dot{q}) + \Delta b(q,\dot{q}) \qquad (20)$$

where $M_n(q)$, $b_n(q,\dot{q})$ and $g_n(q)$ are respectively the nominal inertia matrix, nominal vector of coriolis and centripetal forces and the nominal gravity term. Δ stands for the deviation between these terms and the actual ones. Therefore, using a linearization feedback control law will not entirely cancel out the non-linear terms of (19). Nevertheless, the difference between the nominal and actual plant's dynamics can be considered as disturbance which can be estimated and compensated through an additional control law. Rewriting (19)

$$M(q)\ddot{q} + b_n(q,\dot{q}) + \Delta b(q,\dot{q}) + g_n(q) + \Delta g(q) = \tau(t) \quad (21)$$

Then, the linearization feedback control law $u^{lin}(t)$ can be expressed as

$$u^{lin}(t) = b_n(q,\dot{q}) + g_n(q) \qquad (22)$$

Consequently, using the previous control input in the overall control $\tau(t)$. (19) can be written as follows

$$M_n(q)\ddot{q} + \underbrace{\Delta M(q)\ddot{q} + \Delta b(q,\dot{q}) + \Delta g(q)}_{d(t)} = u(t) \qquad (23)$$

It is commonly believed that the last three terms of (23) can be considered as disturbance signal $d(t)$ [9]. Moreover, it can be estimated through the following low pass filter

$$\widehat{d}(t) = \frac{g}{s+g}[u^{ref}(t) + gM_n(q)\dot{q}] - gM_n(q)\dot{q} \qquad (24)$$

where $g \in \mathrm{R}^+$ is the single observer gain which controls how fast the estimated signal converges to the actual disturbance
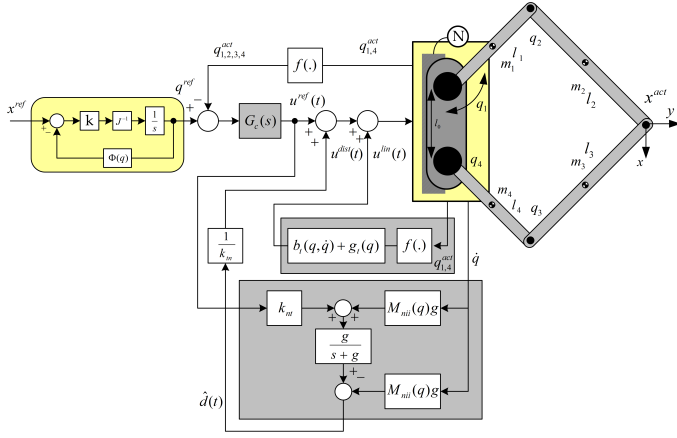
Fig. 5.   Configuration space measurement.

Fig. 6.   Task space measurements.

[10]. Then, the estimated disturbance is used to generate the following control law

$$u^{dist}(t) = \frac{1}{k_{tn}}\widehat{d}(t) \qquad (25)$$

that is used along with the feedback linearization control law (24) to formulate the following overall control law.

$$\tau(t) = u^{lin}(t) + u^{dist}(t) + u^{ref}(t) \qquad (26)$$

Figure (5) illustrates the block diagram implementation of the control law (26) that is composed of three entries. The first is a feedback linearization control law that depends on the nominal plant's dynamics. Therefore, it doesn't entirely cancel out all the nonlinear terms of the parallel robot. However, the second control law generated through disturbance observer in the outer loop of Fig.5 or (24) and (25) is used to cancel out the remainder non-linear terms of (19). The third term u^{ref} is an arbitrary control law. The non-linear function $f(.)$ represents a kinematical equation that relates the pantograph's passive angles with its active angles.

2) Task space measurements: Rewriting (19) in the task space

$$M_t(q)\ddot{\mathrm{x}} + b_t(q,\dot{q}) + g_t(q) = F_t(t) \qquad (27)$$

that can be obtained through the following mappings

$$\begin{aligned} M_t(q) &= (\mathrm{J}^\dagger)^{\mathrm{T}}M(q)\mathrm{J}^\dagger \\ b_t(q,\dot{q}) &= (\mathrm{J}^\dagger)^{\mathrm{T}}b(q,\dot{q}) - M_t(q)\mathrm{J}\dot{q} \\ g_t(q) &= (\mathrm{J}^\dagger)^{\mathrm{T}}g(q) \ , \ \tau(t) = \mathrm{J}^{\mathrm{T}}F_t \end{aligned} \qquad (28)$$

where, $F_t(t)$ and $\mathrm{J}^\dagger$ are the task space force vector and the jacobian matrix pseudo-inverse, respectively. Similar to the kinematical uncertainties argument, (27) can be rewritten taking the following dynamical uncertainties into consideration

$$M_t(q)\ddot{\mathrm{x}} + b_{tn}(q,\dot{q}) + \Delta b_t(q,\dot{q}) + g_{tn}(q) + \Delta g_t(q) = F_t(t) \quad (29)$$

similarly, the linearization feedback control law is

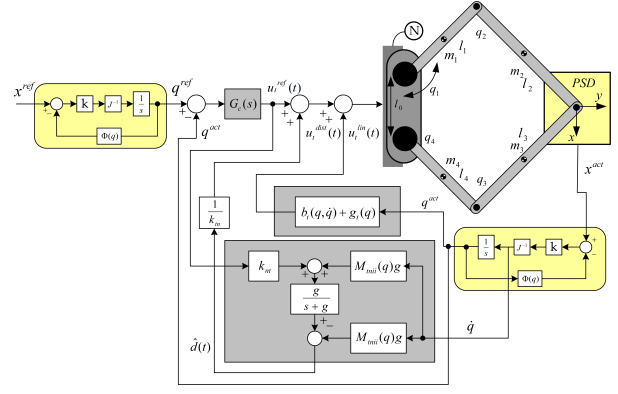$$u_t^{lin}(t) = b_{tn}(q,\dot{q}) + g_{tn}(q) \qquad (30)$$

Since measurements are taken from the task space, the disturbance observer structure can be modified as follows

$$\widehat{d}_t(t) = \frac{g}{s+g}[u_t^{ref}(t) + gM_{tn}(q)\mathrm{J}\dot{\mathrm{x}}] - gM_{tn}(q)\mathrm{J}\dot{\mathrm{x}} \quad (31)$$

$$u_t^{dist}(t) = \frac{1}{k_{tn}}\widehat{d}_t(t) \qquad (32)$$

$$F_t(t) = u_t^{lin}(t) + u_t^{dist}(t) + u_t^{ref}(t) \qquad (33)$$

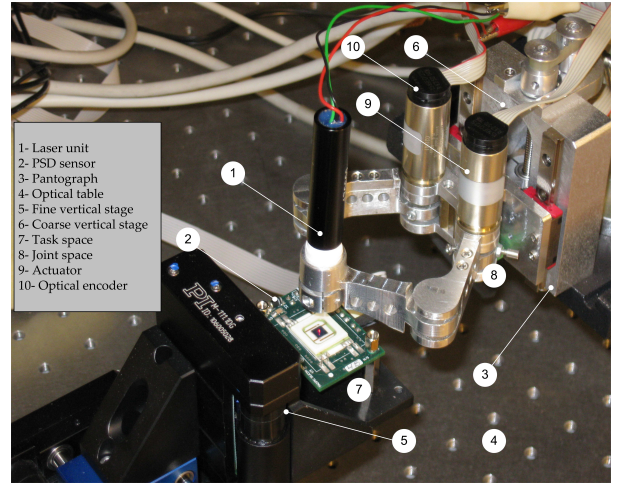Block diagram implementation of the previous control law

Fig. 7.   Experimental setup.

is illustrated in Fig.6 where measurement of the pantograph's end effector is taken through a position sensing device which provides the controller with the end effector's actual position regardless to any kinematical or dynamical inaccuracies. However, the configuration space equation of motion has to be mapped to the task space that can be performed through (28).

IV. EXPERIMENTAL RESULTS

In order to investigate the influence of task and configuration space measurements on the precision of a motion control
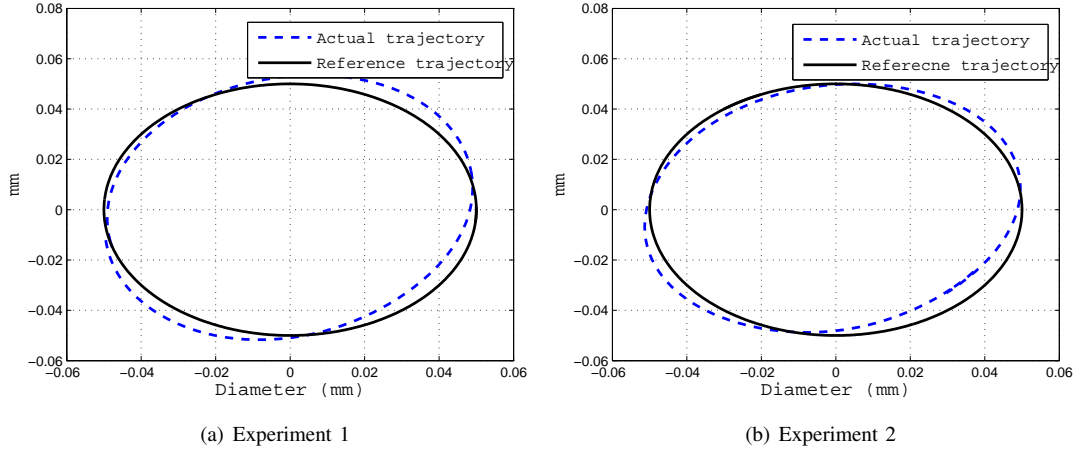
(a) Experiment 1   (b) Experiment 2

Fig. 8. 100 μm circles reference and actual trajectory (configuration space measurements).
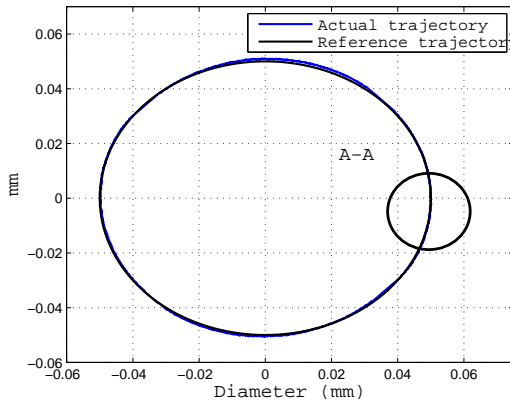
operation in the presence of both kinematical and dynami-cal inaccuracies, experiments are conducted using both task space and configuration space measurements. The experimen-tal setup consists of a parallel robot namely, pantograph. The pantograph's nominal kinematical and dynamical parameters are included in Table.I. The five linkage mechanism is driven with two actuators where their encoders are used as sensors for the configuration space control while the task space control is performed using a PSD sensor with 1 μm resolution, mounted on the bottom of the pantograph's end effector which by its turn holds a laser unit that directs a laser beam on the optical sensor as depicted in Fig.7.

First, experiments are conducted using measurements taken from the actuator's optical encoder with 512 pulse/rev resolu-tion. Figure (8) illustrates the experimental result for a circular trajectory with 100 μm diameter. Although the control process was performed over the configuration space measurement, the end effector actual position was measured using the task space PSD sensor so as to verify whether the kinematical inaccuracies that experience has proven to be unavoidable will severely affect the performance. Indeed, Fig.8 indicates a pioneer difference between the actual measurement and the desired 100 μm diameter circular trajectory. However, such difference was expected as the entire parallel robot is placed outside the control loop due to the nature of the configuration space measurement. The control signal has a direct effect on the robot's active angles, On the other hand, the steady state error due to the kinematical inaccuracies cannot be compensated by this control action which only guarantees that the robot's active angles follow a pre-specified reference trajectories that can be also concluded from (7) where the control action has no effect on the steady state error developed by the unavoidable kinematical inaccuracies. It has been shown through (11) that merging measurements from configuration space to the task space decreases control system's sensitivity to kinematical inaccuracies while disturbance estimation and rejection decrease control system's sensitivity to dynamical inaccuracies. However, measuring the end effector's exact
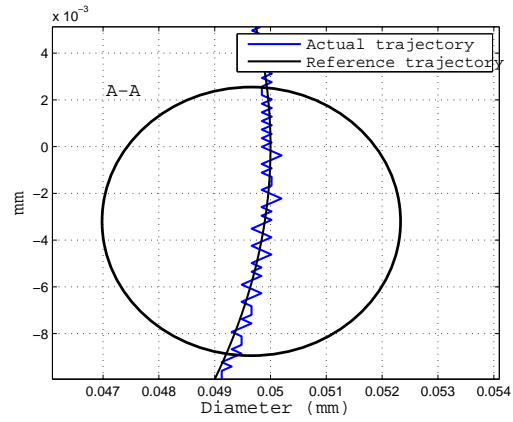
position requires utilization of a position sensing device as depicted in Fig.7. End effector's actual cartesian position is then mapped into joint space coordinates through (14). The obtained coordinates are then subtracted from the reference ones to generate a vector of error signal. At this stage the kine-matical inaccuracies associated with both the actual mapped coordinates and the desired coordinates due to transformation (14) are canceled out that can also be interpreted through (18). Experimentally, each of the pantograph's active angle is independently controlled through task space measurement. Figure (9) illustrates the result of controlling the pantograph's end effector during a circular trajectory tracking assignment. Pantograph's end effector is indeed tracking the circular tra-jectory regardless to the kinematical inaccuracies associated with each of the planar mechanism's element. The kinematical errors exist in every element, in every manufacturing step, in every assembly action in addition to the active deviations that arise due to thermal deformations when the mechanism is put into action in an out of the laboratory environment. Nevertheless, the control system is unsensitive to any of these kinematical inaccuracies as measurements are merged from the joint to task space. In other words, kinematical inaccuracies are included inside the control closed loop rather than keeping them outside when measurements are taken from the active joints. A magnified plot of the obtained end effector's response is illustrated in Fig.9-b which demonstrates that the controlled end effector is trying to follow a pre-specified trajectory in the presence of unavoidable non-negligible inaccuracies. In addition, a circular trajectory of 50 μm radius is followed so as to demonstrate the enhanced capability of the control system when measurements are merged to the task space. Figure (9)-b shows undesired oscillatory response along the reference trajectory due to the utilized simple independent joint control. However, better response can be obtained through (33).

V. CONCLUSION

This work demonstrates that merging measurements to task space in order to obtain end effector's exact position reduces

(a) Experiment 1

(b) Magnified plot

Fig. 9.   100 μm circles reference and actual trajectory (task space measurements).

control system's sensitivity to any kinematical or dynamical inaccuracies. Consequently, the regular calibration process becomes unnecessary at all even when performing high precision motion control. In addition, this work demonstrates that merging the measurements to the task space along with disturbance observer makes the control system unsensitive to both kinematical and dynamical uncertainties. In other words, control system's sensitivity to kinematical inaccuracies is reduced by measuring the end effector's actual position rather than having it computed through mapping which depends on uncertain entries while control system's sensitivity to dynamical inaccuracies is reduced through both feedback linearization and disturbance compensation. Feedback linearization cancels out modeled dynamics to certain level along the entire frequency range of the parallel robot while disturbance observer cancels out the rest of the unmodeled dynamics and what feedback linearization failed to cancel out that is however limited on the parallel robot's low frequency range due to disturbance observer's sensitivity function. In order to verify the validity of the proposed control framework, experiments are conducted on a planar parallel robot with kinematical inaccuracies, manufacturing tolerances and assembly errors. In addition, the end effector is supposed to follow a circular trajectory with 50 μm radius. Comparison between results obtained when measurements are taken from the joint and task spaces demonstrate that the last one is unsensitive to kinematical inaccuracies that in turn demonstrates that measurements nature have more impact on end effector's motion accuracy while other aspects including enhancement of machining accuracy and reducing assembly errors are not only hard to achieve but also extremely costly especially when accurate positioning is required. Experimental results proved the feasibility of the proposed control framework without performing any calibration to the parallel robot.

ACKNOWLEDGMENT

TABLE I
EXPERIMENTAL PARAMETERS.

Parameter	Value	Parameter	Value
l_{1n}, l_{2n}	0.04 m	g	628 rad/s
l_{3n}, l_{4n}	0.04 m	g_{lpf}	314 rad/s
l_{on}	0.03 m	J_{mn}	0.4 $g.cm^2$
k_{tn}	8.26 mNm/A	k_{bn}	0.865 mv/rpm

REFERENCES

[1] F. Pacot, P. Lemoine, N. Andreff, D. Chablat and P. Martinet, "A Vision-based Computed Torque Control for Parallel Kinematic Machines," in *Proc Int. Conf. ICRA08 International Conference on Robotics and Automation., 2008*, vol. 1, pp. 1556-1561, May. 2008.

[2] D. Yu and J. Han, "Kinematic Calibration of Parallel Robots," in *Proc Int. Conf. ICMA05 International Conference on Mechatronics and Automation., 2005*, vol. 1, pp. 521-525, July. 2005.

[3] G. Campion, Q. Wang and V. Hayward, "The Pantograph MK-II: A Haptic Instrument," in *Proc Int. Conf. IROS05 International Conference on Intelligent Robots and Systems., 2005*, vol. 1, pp. 723-728, 2005.

[4] T. Ropponen and T. Arai, "Accuracy Analysis of a Modified Stewart Platform Manipulator," in *Proc Int. Conf. ICRA95 International Conference on Robotics and Automation., 2008*, vol. 1, pp. 521-525, 1995.

[5] P. Maurine and E. Dombre, "A Calibration Procedure For The Parallel Robot Delta 4," in *Proc Int. Conf. ICRA96 International Conference on Robotics and Automation., 1996*, vol. 1, pp. 975-980, April. 1996.

[6] Q. Ding, L. Sun, J. Ji and L. Zhang "Calibration of A 2-DOF Planar Parallel Robot: Home Position Identification and Experimental Verification," in *Proc Int. Conf. ICMA05 International Conference on Mechatronics and Automation., 2005*, pp. 510-515, July. 2005.

[7] Y. Lingtao, W. Jian, D. Zhijiang, S. Lining and C. Hegao "A Novel Method on Parallel Robot's Pose measuring and Calibration," in *Proc Int. Conf. ICIEA07 International Conference on Industrial Electronics and Applications., 2007*, pp. 1292-1296, 2007.

[8] K. Ohnishi, M. Shibata and T. Murakami, "Motion Control for Advanced Mechatronics", *ASME Transaction On Mechatronics*, vol. 1, no. 1, pp. 56-67, March. 1996.

[9] T. Murakami and K. Ohnishi, "Observer-Based Motion Control-Application to Robust Control and Parameter Identification," in *Proc Int. Conf. IEEE Industrial Electronics Society., Nov, 1993*, vol. 1, pp. 1-6.

[10] S. Katsura and K. Ohnishi, "Force Servoing by Flexible Manipulator Based on Resonance Ratio Control," *IEEE Transaction On Industrial Electronics*, vol. 54, no. 1, pp. 56-67, February. 2007.